# Thickness-driven antiferroelectric-to-ferroelectric phase transition of thin $PbZrO_3$ layers in epitaxial $PbZrO_3/Pb(Zr_{0.8}Ti_{0.2})O_3$ multilayers

Ksenia Boldyreva[a)]
*Max Planck Institute of Microstructure Physics, Weinberg 2, D-06120 Halle (Saale), Germany*

Lucian Pintilie
*Max Planck Institute of Microstructure Physics, Weinberg 2, D-06120 Halle (Saale), Germany and NIMP, P.O. Box MG-7, 077125 Bucharest-Magurele, Romania*

Andriy Lotnyk, I. B. Misirlioglu, Marin Alexe, and Dietrich Hesse
*Max Planck Institute of Microstructure Physics, Weinberg 2, D-06120 Halle (Saale), Germany*

(Received 31 July 2007; accepted 31 August 2007; published online 21 September 2007)

Epitaxial antiferroelectric/ferroelectric $PbZrO_3/PbZr_{0.8}Ti_{0.2}O_3$ multilayers were grown on $SrRuO_3$-electroded $SrTiO_3(100)$ substrates by pulsed laser deposition. Polarization-field and switching current-voltage curves show a mixed antiferroelectric-ferroelectric behavior of the multilayers with an individual layer thickness above 10 nm, whereas below 10 nm the multilayers show only ferroelectric behavior. Clearly the $PbZrO_3$ layers thinner than 10 nm experienced a transition into the ferroelectric state. X-ray diffraction reciprocal space mapping showed a corresponding orthorhombic-to-rhombohedral transition of the $PbZrO_3$ layers. The observations are discussed in terms of the influence of strain. © *2007 American Institute of Physics*.
[DOI: 10.1063/1.2789401]

Epitaxial perovskite-type multilayers such as $PbZrO_3/BaZrO_3$, $PbTiO_3/PbZrO_3$, $BaTiO_3/SrTiO_3$, $SrTiO_3/BaZrO_3$, or $Pb(Zr_xTi_{1-x})O_3/Pb(Zr_yTi_{1-y})O_3$, represent a class of interesting systems with enhanced ferroelectric or dielectric properties.[1–8] Strain and coupling effects between individual layers can result in qualitatively new properties.[1,8–11] For example, Kanno *et al.*[3] reported that the dielectric constant of $PbZrO_3/PbTiO_3$ epitaxial multilayers increases with decreasing thickness of the component layers for the same total thickness of the structure. This behavior was considered a consequence of the interlayer strain and electrical interaction of the dipoles at the interfaces. On the other hand, the hysteresis loop looks like for a ferroelectric material no matter the thickness of the component layers is five unit cells (~2 nm) or 100 unit cells (~40 nm). Studies on sol-gel grown, polycrystalline $Pb(Zr_xTi_{1-x})O_3/PbZrO_3$ multilayers in dependence on the annealing conditions were limited to some qualitative observations.[12]

We report on growth, structure and layer thickness-dependent properties of epitaxial $PbZrO_3/Pb(Zr_{0.8}Ti_{0.2})O_3$ (PZO/PZT) multilayers with a PZO/PZT ratio of 1:1. The multilayers were prepared by pulsed laser deposition on (100)-oriented vicinal $SrTiO_3$ (STO) substrates, using a KrF excimer laser at a wavelength of 248 nm. The STO substrates were chemically and thermally treated in order to achieve step-terrace structures with only one unit-cell height.[13] A conducting $SrRuO_3$ (SRO) epitaxial bottom electrode was used. A 5 nm thick tetragonal $Pb(Zr_{0.2}Ti_{0.8})O_3$ buffer layer was deposited on top of the SRO electrode to reduce the misfit between the rhombohedral PZT and its underlayer. The deposition temperature was set at 575 °C for all layers, with an oxygen pressure of 0.1 mbar for PZO and rhombohedral PZT, 0.14 mbar for SRO, and 0.2 mbar for the tetragonal PZT buffer layer during deposition. The laser fluence was set to 1.5, 0.9, 1.0, and 1.0 $J/cm^2$ for depositing PZO, SRO, PZT, and the tetragonal buffer layer, respectively. Pt top electrodes were deposited through a stainless steel shadow mask by rf sputtering. Samples for transmission electron microscopy (TEM) were thinned using mechanical and ion-beam based standard methods. TEM investigations were performed in a Philips CM20T at 200 kV. X-ray diffraction (XRD) $\theta$-$2\theta$ scans and reciprocal space mappings (RSMs) were performed on a Philips X'Pert MRD diffractometer with Cu $K\alpha$ radiation. Polarization-voltage (P-V) hysteresis loops and switching current-voltage (*I-V*) characteristics of the multilayers were recorded by an AixAcct thin film analyzer 2000. The surface morphology of the multilayers was characterized by atomic force microscopy (AFM), revealing layer-by-layer growth resulting in stepped terraces (not shown).

Structure and properties of single-phase antiferroelectric (AFE) orthorhombic PZO (lattice parameters $a=5.88$ Å, $b=11.787$ Å, and $c=8.231$ Å) and ferroelectric (FE) rhombohedral PZT (lattice parameters $a=4.118$ Å and $\alpha=89.73°$) thin films (and single crystals) are well known.[14–20] Whereas the ferroelectric PZT films show the well-known polarization-field hysteresis loop, a characteristic double loop is recorded from antiferroelectric PZO films due to a field-induced antiferroelectric-to-ferroelectric transition. During this transition the crystallography of PZO changes from orthorhombic to rhombohedral.[21]

Three sets of samples $(PZO_t/PZT_t)_m$ with the overall thicknesses $T$ of 50, 100, and 150 nm, respectively, were studied, where $t$ is the thickness (in nanometers) of the individual PZO or PZT layers, and $m$ is the number of PZO/PZT bilayers. The results were quite similar for the three sets of samples. The structure of a multilayer with $T=100$ nm and $m=4$ is shown in Fig. 1. The TEM contrast between PZO and PZT layers is rather weak due to the structural similarity and the rather small difference in composition. All the layers

[a)]Electronic mail: ksenia@mpi-halle.de

 

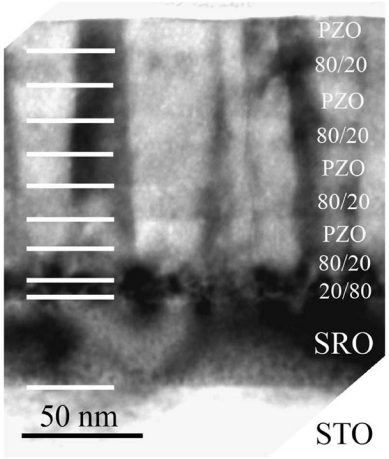


FIG. 1. TEM cross-section micrograph of a multilayer with 100 nm overall thickness and with four bilayers and a thickness of the individual layers of 12.5 nm.

grow epitaxially in the $(001)_{pc}$ orientation (pc-pseudocubic), as revealed by electron diffraction (not shown).

The hysteresis curves of $(PZO_t/PZT_t)_m$ multilayers with $T=100$ nm, but different number $m$ of bilayers ($m=1$, 2, 4, 6, and 8), corresponding to $t=50$, 25, 12.5, ~9, and ~6 nm, respectively, were recorded. The samples with $t=50$, 25, and 12.5 nm show a mixed FE-AFE behavior, whereas the samples with $t=9$ and 6 nm show only FE behavior. Figure 2(a) shows the hysteresis loops for the extreme $t$ values of 50 and 6 nm. The mixed FE-AFE behavior in the case of $t=50$ nm is clearly visible in the switching $I$-$V$ curve shown in Fig. 2(b). Two additional switching peaks (encircled) occur around zero bias, in addition to the four major switching peaks corresponding to the AFE double loop. The sample with $t=6$ nm, however, shows only the two peaks, as it should be in the case of purely FE behavior. In other words, the multilayers undergo a thickness-related transition from a mixed AFE-FE behavior to a purely FE behavior. This is in contradiction to the previous report on $PbZrO_3/PbTiO_3$ epitaxial multilayers, which shows only ferroelectric behavior independent of the thickness of the individual layers.[3] It

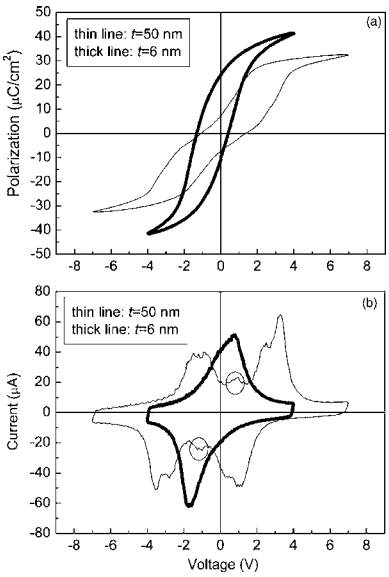


FIG. 2. (a) Hysteresis and (b) switching current-voltage curves for the PZO/PZT multilayers with $t=50$ nm and $t=6$ nm.

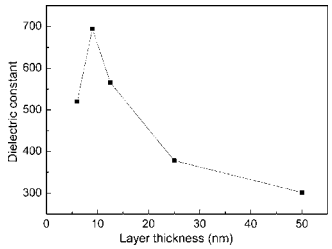


FIG. 3. Dependence of the dielectric constant on the thickness of the individual layers in the epitaxial PZO/PZT multilayers.

should be pointed out, however, that we had performed an extensive optimization of the deposition conditions for PZO layers.[15]

Similar to the temperature-driven phase transitions, where the dielectric constant increases at the critical temperature, some sudden increase of the dielectric constant may be expected at a critical thickness in the case of a thickness-driven phase transition. Therefore, we measured the capacitance at zero bias, and represented the calculated dielectric constant as a function of $t$ (Fig. 3). As expected, there is a maximum at a thickness of 9–10 nm suggesting that this is the critical thickness $t_c$ for the phase transition.

Figure 4(a) shows part of a $\theta$-$2\theta$ XRD scan of two samples, viz., $t=25$ nm and $t=6$ nm. Whereas the former sample shows two distinct peaks at $2\theta=95.35°$ ($d$ value of 1.0419 Å) and 96.42° ($d$ value of 1.0331 Å) corresponding to the PZO $(480)_0$ and PZT (004) reflections, respectively, the latter sample shows only one peak at $2\theta=96.11°$ ($d$ value of 1.0356 Å), which corresponds to a somewhat strained, uniformly rhombohedral phase. This means that PZO has undergone a structural phase transition from orthorhombic to rhombohedral, which is equivalent to the observed antiferroelectric-to-ferroelectric transition. This is even more clearly illustrated by the RSM plots shown in Figs. 4(b) and 4(c), where the sample with $t=25$ nm shows two peaks, one for orthorhombic PZO and one for rhombohedral PZT, and the one with $t=6$ nm shows only one peak very close to the position of the rhombohedral peak of the first sample. In a pseudocubic approximation (see Ref. 22), the sample with $t=25$ nm consists of PZO layers with $a_{pc}=4\times1.0419$ Å=4.17 Å and PZT layers with $a_{pc}=4\times1.0331$ Å=4.13 Å, so that the PZO is under compressive, the PZT under tensile strain. After the structural phase transition both phases have $a_{pc}=4\times1.0356$ Å=4.14 Å, indicating that strain plays an important role as an origin of the thickness-driven antiferroelectric-to-ferroelectric transition of the PZO layers.

Discussing this transition, one should keep in mind that the component materials of the multilayer have different paraelectric-to-(anti)ferroelectric transition temperatures. As a consequence, they experience successive phase transitions of this type as the stack is cooled down from the deposition temperature of 575 °C. During growth, all the layers have a cubic structure. Considering for simplicity the transition temperatures for the bulk, we expect that the para-to-ferro (cubic-to-rhombohedral) transition of the (Zr-rich) PZT layers occurs at 317 °C, and the para-to-antiferro (cubic-to-orthorhombic) transition of the PZO layers at 230 °C. A modification of the strain and electrical boundary conditions for each of the layers results at every transition temperature. In particular, in the temperature range between the transition of the (Zr-rich) PZT and that of PZO, the PZO layers are

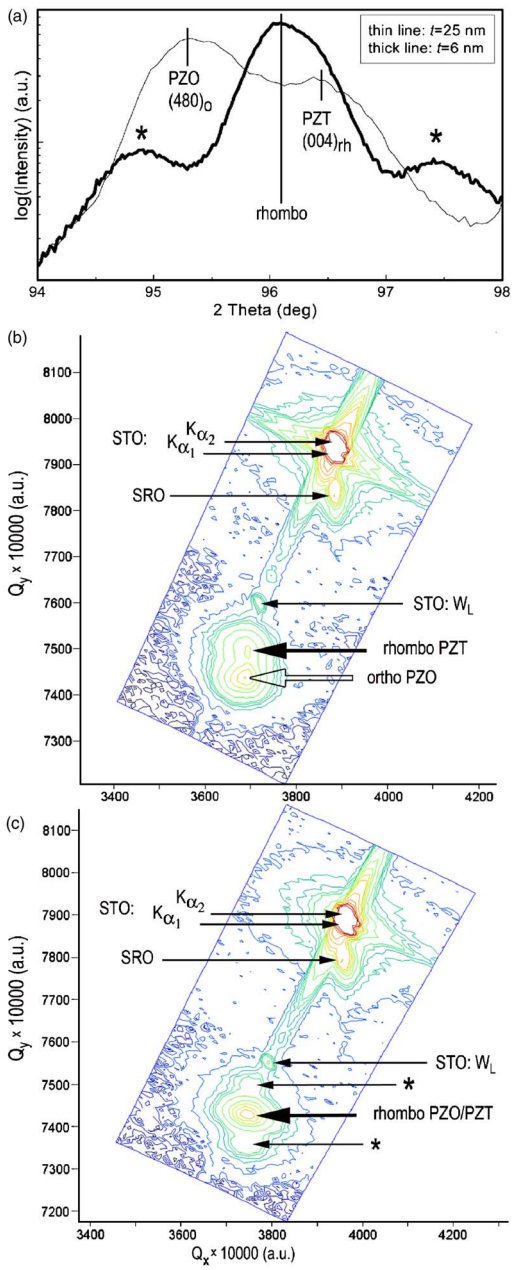


FIG. 4. (Color online) (a) XRD $\theta$-$2\theta$ scan ($\psi$=0°) and [(b) and (c)] RSM plots around the (402) reflection of STO ($\psi$=26.6°) of a sample with $t$=25 nm [(a) and (b)] and one with $t$=6 nm [(a) and (c)]. The two peaks marked with an asterisk in (a) and (c), which are on an equal distance of $\Delta(2\theta)$=1.3° from the PZT(400) peak, are second-order superlattice reflections indicating a PZO/PZT layer period of 13.4 nm. $Q_x$ and $Q_y$ in (b) and (c) are the $x$ and $y$ components of the reciprocal space vector: a.u.—arbitrary units. Diffraction from the $Pb(Zr_{0.2}Ti_{0.8})O_3$ buffer layer is not seen due to the low thickness of this layer.

expected to be cubic and paraelectric, whereas the PZT layers are already rhombohedral and ferroelectric. The corresponding polarization charge at the interfaces may induce a nonzero electric field in the PZO layers in addition to the strain. Possibly this field helps to drive the PZO layers toward the rhombohedral, ferroelectric phase. This shows that the operating mechanism may be complex and not just due to interfacial strain. However, strain should play an important role: It is well known that the FE phase in PZO thin films or single crystals can be easily induced also by stress[14,23] due to the small free energy difference between the FE and the AFE states.[24] More investigations, including also Monte Carlo simulations, are underway to clarify the details of the mechanism of the thickness-induced phase transition.

In conclusion, a thickness-driven antiferroelectric-to-ferroelectric, orthorhombic-to-tetragonal phase transition of the $PbZrO_3$ layers in epitaxial antiferroelectric/ferroelectric $PbZrO_3/PbZr_{0.8}Ti_{0.2}O_3$ multilayers has been observed at a $PbZrO_3$ thickness below 10 nm. This transition is most probably a consequence of the particular strain built up at the interfaces during cooling down after growth.

Thanks are due to M. A. Schubert for help with XRD. One of the authors (I.B.M.) thanks the Alexander von Humboldt Foundation for funding.

[1]T. B. Wu and C. L. Hung, Appl. Phys. Lett. **86**, 112902 (2005).
[2]T. Choi and J. Lee, Thin Solid Films **475**, 283 (2005).
[3]I. Kanno, S. Hayashi, R. Takama, and T. Hirao, Appl. Phys. Lett. **68**, 328 (1996).
[4]T. Harigai, D. Tanaka, H. Kakemoto, S. Wada, and T. Tsurumi, J. Appl. Phys. **94**, 7923 (2003).
[5]J. Kim, Y. Kim, Y. S. Kim, J. Lee, L. Kim, and D. Jung, Appl. Phys. Lett. **80**, 3581 (2002).
[6]H. M. Christen, E. D. Specht, S. S. Silliman, and K. S. Harshavardhan, Phys. Rev. B **68**, 020101 (2003).
[7]F. M. Pontes, E. Longo, E. R. Leite, and J. A. Varela, Appl. Phys. Lett. **84**, 5470 (2004).
[8]I. Vrejoiu, Y. L. Zhu, G. Le Rhun, M. A. Schubert, D. Hesse, and M. Alexe, Appl. Phys. Lett. **90**, 072909 (2007).
[9]A. L. Roytburd, S. Zhong, and S. P. Alpay, Appl. Phys. Lett. **87**, 092902 (2005).
[10]I. B. Misirlioglu, G. Akcay, S. Zhong, and S. P. Alpay, J. Appl. Phys. **101**, 036107 (2007).
[11]J. Zhai, X. Yao, and L. Zhang, Ceram. Int. **30**, 1263 (2004).
[12]S. H. Bae, K. B. Jeon, and B. M. Jin, Mater. Res. Bull. **36**, 1931 (2001); S. H. Bae, K. B. Jeon, B. M. Jin, and I. W. Kim, Ferroelectrics **260**, 113 (2001); S. H. Bae, K. B. Jeon, S. C. Kim, and B. M. Jin, *ibid.* **260**, 131 (2001); S. H. Bae, K. B. Jeon, and B. M. Jin, *ibid.* **328**, 9 (2005).
[13]G. Koster, B. L. Kropman, G. J. H. M. Rijnders, D. H. A. Blank, and H. Rogalla, Appl. Phys. Lett. **73**, 2920 (1998).
[14]M. P. Moret, J. J. Schremer, F. D. Tichelaar, E. Aret, and P. R. Hageman, J. Appl. Phys. **92**, 3947 (2001).
[15]K. Boldyreva, D. Bao, G. Le Rhun, L. Pintilie, M. Alexe, and D. Hesse, J. Appl. Phys. **102**, 044111 (2007).
[16]D. Viehland, Phys. Rev. B **52**, 778 (1995).
[17]D. L. Corker, A. M. Glazer, R. W. Whatmore, A. Stallard, and F. Fauth, J. Phys.: Condens. Matter **10**, 6251 (1998).
[18]S. K. Streiffer, C. B. Parker, A. E. Romanov, M. J. Lefevre, L. Zhao, J. S. Speck, W. Pompe, C. M. Foster, and G. R. Bai, J. Appl. Phys. **83**, 2742 (1998).
[19]K. Tokita, M. Aratani, and H. Funakubo, Ferroelectrics **260**, 45 (2001).
[20]D. I. Woodward, J. Knudsen, and I. M. Reaney, Phys. Rev. B **72**, 104110 (2005).
[21]O. E. Fesenko, R. V. Kolesova, and Yu. G. Sindeyev, Ferroelectrics **20**, 177 (1978).
[22]F. Jona, G. Shirane, F. Mazzi, and R. Pepinsky, Phys. Rev. **105**, 849 (1957).
[23]V. Yu. Topolov, A. V. Turik, O. E. Fesenko, and V. V. Eremkin, Ferroelectr., Lett. Sect. **20**, 19 (1995).
[24]E. Sawaguchi, J. Phys. Soc. Jpn. **81**, 615 (1953).